Applied Catalysis A: General 490 (2015) 133–138

Contents lists available at ScienceDirect

Applied Catalysis A: General

journal homepage: www.elsevier.com/locate/apcata

PtAu/C electrocatalysts as anodes for direct ammonia fuel cell

Júlio César M. Silva, Sirlane G. da Silva, Rodrigo F.B. De Souza, Guilherme S. Buzzo, Estevam V. Spinacé, Almir O. Neto, Mônica H.M.T. Assumpção *

Instituto de Pesquisas Energéticas e Nucleares, IPEN/CNEN-SP, Av. Prof. Lineu Prestes, 2242 Cidade Universitária, CEP 05508-900, São Paulo, SP, Brazil

ARTICLE INFO

Article history:
Received 24 June 2014
Received in revised form 5 November 2014
Accepted 11 November 2014
Available online 18 November 2014

Keywords:
PtAu/C catalysts
Ammonia oxidation
Direct ammonia fuel cell.

ABSTRACT

PtAu/C electrocatalysts prepared by borohydride reduction method with different Pt:Au atomic ratios (50:50 and 70:30) were tested as work electrodes/anodes in electrochemical experiments and also using a direct ammonia fuel cell (DAFC). X-ray diffraction patterns showed the formation of PtAu alloy while transmission electron micrographs showed the particles sizes between 5.8 and 6.4 nm. PtAu/C 70:30 presented the best results showing a current density about 20% higher when compared to Pt/C in voltammetry experiments and a power density about 60% higher than Pt/C using DAFC, while Au/C showed practically no activity in both experiments. The best results obtained with PtAu/C (70:30) could be explained by the electronic effect (PtAu alloy) associated with adsorbed hydroxyl species ($AuOH_{ads}$) and also the lower Au-N energy adsorption.

1. Introduction

Global warming worries and the continuous and fast depletion of fossil fuels have led scientists to look for substantial improvement in energy conversion efficiencies. Moreover, the increase in the concentration of greenhouse gases, have also contribute to the development of new alternatives and 'greener' energy sources. As a result, fuel cells have generated a lot of interest in the scientific and engineering communities [1,2].

Among the different types of fuel cells, the alkaline fuel cells (AFCs) have numerous advantages over proton exchange membrane fuel cells on both cathode kinetics and ohmic polarization since the less-corrosive nature of an alkaline environment ensures a potential greater longevity and the kinetics of the oxygen reduction reaction (ORR) is more facile in alkaline media than in acid [3].

One of the most used fuels in fuel cells is the hydrogen. Although H_2 is usually the preferred choice of fuel as high power densities can be obtained, effective and economical production and storage of hydrogen as well as its refueling infrastructure are still facing major challenges [4]. It is therefore necessary the use of alternative fuels.

Among the useful fuels is ammonia, liquid ammonia is an excellent low-temperature fuel since it has 70% more hydrogen content and 50% higher specific energy density than liquid hydrogen per unit volume. Additionally, ammonia is a perfect H_2 carrier because it holds 18% hydrogen by mass, it is easy to store, has a worldwide distribution infrastructure, it is CO free and it is stable [5–10].

Furthermore, it is known that there are a lot of chemical processes that use ammonia as reactant or produce ammonia as by-product. Thus, the removal of ammonia from waste steams is becoming an increasingly important issue [11]. Then, several studies have been devoted to the development of efficient electrocatalysts for ammonia electro-oxidation in alkaline solutions; however, until now platinum is the most active catalyst for this process [5,12–14].

Lomocso and Baranova [12] developed different carbon supporting PtM nanoparticles (M = Ir, Pd, SnO_x) and showed that the binary synthetized materials present more electro-catalytic activity toward ammonia electro-oxidation when compared to Pt/C, however the conclusions were obtained just by electrochemical experiments.

More recently out research group evaluated the use of PtIr/C [15] and PdIr/C [16] electrocatalysts toward ammonia oxidation taking into account DAFC experiments and among them PtIr/C electrocatalysts yields more promissory materials than PdIr/C although the conditions were quite different.

Considering the use of binary catalysts toward ammonia oxidation Au could be a good alternative to be combined with Pt since Au shows lower N adsorption energy than Pt. Thus, Au could contribute to the decrease of poisoning on catalysts surface by N_{ads} species, facilitating the ammonia oxidation [12,17,18].

Aiming the development of direct ammonia fuel cells (DAFCs) the present study describes the use of different PtAu/C

* Corresponding author. Tel.: +55 11 3133 9284.
E-mail address: monica_ucri@yahoo.com.br (M.H.M.T. Assumpção).

http://dx.doi.org/10.1016/j.apcata.2014.11.015
0926-860X/

compositions (50:50 and 70:30) contemplating not only electrochemical experiments realized using NH_4OH 1 mol L^{-1} and KOH 1 mol L^{-1}, but also DAFC experiments by using 1, 3 and 5 mol L^{-1} NH_4OH in 1 mol L^{-1} KOH as fuels. It is important to stress that just few studies contemplate the real fuel cell conditions of operation when the issue is the use of ammonia.

2. Experimental

PtAu/C electrocatalyts (20 wt% of metal loading) with different atomic ratios: PtAu/C (50:50) and PtAu/C (70:30), Au/C and Pt/C, were prepared by the borohydride reduction process [19,20] using $H_2PtCl_6{\cdot}6H_2O$ (Aldrich) and $HAuCl_4{\cdot}3H_2O$ (Aldrich), as metal sources. By this process, Vulcan XC72 was firstly dispersed in an isopropyl alcohol/water solution (50/50, v/v) and the mixture homogenized under stirring. After that, the metals sources were added and put on an ultrasonic bath for 5 min and then a solution of $NaBH_4$ in 0.1 mol L^{-1} KOH was added in one portion under stirring and room temperature being the resulting solution maintained under stirring for 15 min. After this procedure, the final mixture was filtered and the solids washed with distillated water and dried at 70 °C for 2 h.

The electrocatalysts were firstly characterized by X-ray diffraction (XRD) using a Rigaku diffractometer model Miniflex II using Cu Kα radiation source (0.15406 nm), being the X-ray diffraction patterns recorded in the range of 2θ =20° to 90° with a step size of 0.05° and a scan time of 2 s per step. Transmission electron microscopy (TEM) images were also carried out using a JEOL transmission electron microscope model JEM-2100 operated at 200 kV.

Electrochemical experiments were conducted at room temperature by cyclic voltammetry at 20 mV s^{-1} in 1 mol L^{-1} KOH and in presence and absence of 1 mol L^{-1} NH_4OH and also by chronoamperometry at −0.300 V for 1000s [21]. For these experiments a regular three-electrode cell was employed using a glassy carbon (geometric area of 0.031 cm^{-2}) as support for work electrodes and a Pt and an HgHgO as counter and reference electrodes, respectively. Working electrodes were constructed by dispersing 8 mg of each powder in a solution composed of 1 mL of water and 40 μL of a 5% Nafion® solution. This mixture was then transferred to an ultrasonic bath for 15 min to produce "black inks". Then 5 μL of the ink was transferred to the glassy carbon support and dried in infrared light. As the total geometric area and the quantity of ink deposited onto the glassy carbon electrode were maintained constant for all experiments, the Pt/C and PtAu/C electrocatalysts currents were normalized by gram of Pt while the Au/C electrode was normalized by the amount of Au.

The DAFCs experiments were conducted in a single cell with 5 cm^2 of area. The temperature was set at 40 °C for the fuel cell and 85 °C for the oxygen humidifier. All electrodes were constructed with 1 mg of Pt per cm^2 in the anode or in the cathode excepted for Au/C which contained 1 mg of Au per cm^2. For all experiments a commercial Pt/C (BASF) was used as cathode. The electrocatalysts were painted over a carbon cloth in the form of a homogeneous dispersion prepared using Nafion® solution (5 wt%, Aldrich). After the preparation, the electrodes were hot pressed on both sides of a Nafion® 117 membrane at 125 °C for 3 min under a pressure of 247 kgf cm^{-2}. Prior to use, the membranes were exposed to 6 mol L^{-1} KOH for 24 h as already proposed [15,22]. The fuel, 1.0, 3.0 and 5.0 mol L^{-1} NH_4OH in 1.0 mol L^{-1} KOH, was delivered at 1 mL min^{-1}, and the oxygen flow was regulated at 150 mL min^{-1}. Electrochemical and DAFC experiments were obtained by using a potentiostat/galvanostat PGSTAT 302 N Autolab.

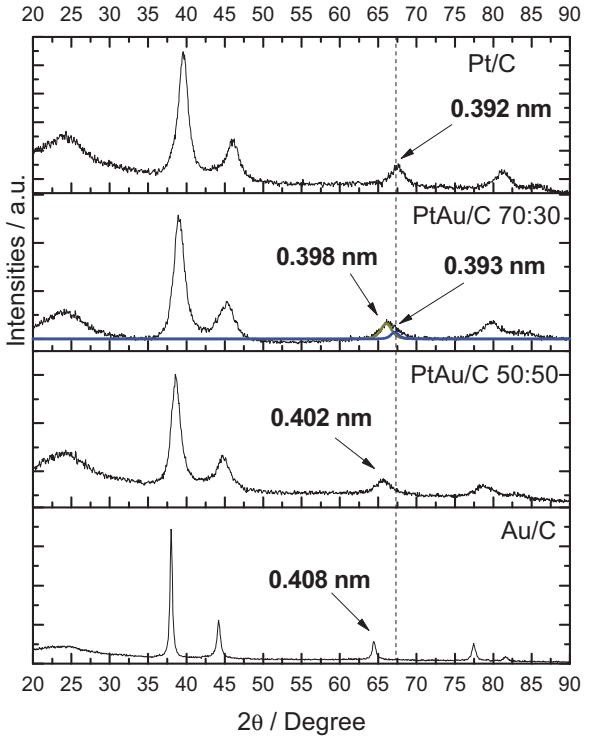

Fig. 1. X-ray diffraction patterns for Au/C, Pt/C and PtAu/C electrocatalysts.

3. Results and discussion

Fig. 1 shows the XRD patterns of the PtAu/C prepared with different atomic ratios and Pt/C and Au/C catalysts prepared by the borohydride reduction process. In all XRD patterns, a broad peak at 2θ about 25° was observed and assigned to the (022) reflection of the hexagonal structure of Vulcan XC 72 carbon [23,24]. The face-centered cubic systems of Pt can also be observed by the peaks at approximately 2θ = 39°, 46°, 67° and 81° [25]. The PtAu/C (70:30) and PtAu/C (50:50) showed the diffractograms shifted to lower values of 2θ when compared to Pt/C, suggesting the formation of PtAu alloy [26]. Thus, the lattice parameters were also calculated for both PtAu materials and the values obtained (inserted in Fig. 1) were higher than the Pt lattice parameter, indicating once more the presence of PtAu alloyed phase. The obtained lattice parameters values are in agreement with the literature [27].

Fig. 2 shows TEM micrographs and histograms of the particle mean diameter distribution for the binary PtAu/C, Pt/C and Au/C catalysts. In all images the particles were well dispersed on carbon support, along with some small particle agglomerations can also be observed. The nanoparticles size were determined by counting about 100 particles at different regions of the different electrocatalysts [28,29] and the particles are with average diameter of 18.5 nm for Au/C, 6.4 nm for PtAu/C (50:50), 5.8 nm for PtAu/C (70:30) and 4.6 nm for Pt/C. Only the Au/C electrocatalyst showed particles higher than 20 nm, with a maximum mean diameter of 77 nm, what is expected since the low melting point of gold results in a difficult preparation of gold catalysts in a highly dispersed state [30,31].

Oko et al. [29] synthetized PtAu nanoparticles and observed that for PtAu (70:30) the nanoparticles average size were lower than for the PtAu (50:50) as observed in the present work. Moreover, they also observed that the positions of the diffraction peaks shifted to lower angles with the increase of Au content and concluded that the variations in the lattice parameters confirm the PtAu alloy formation.

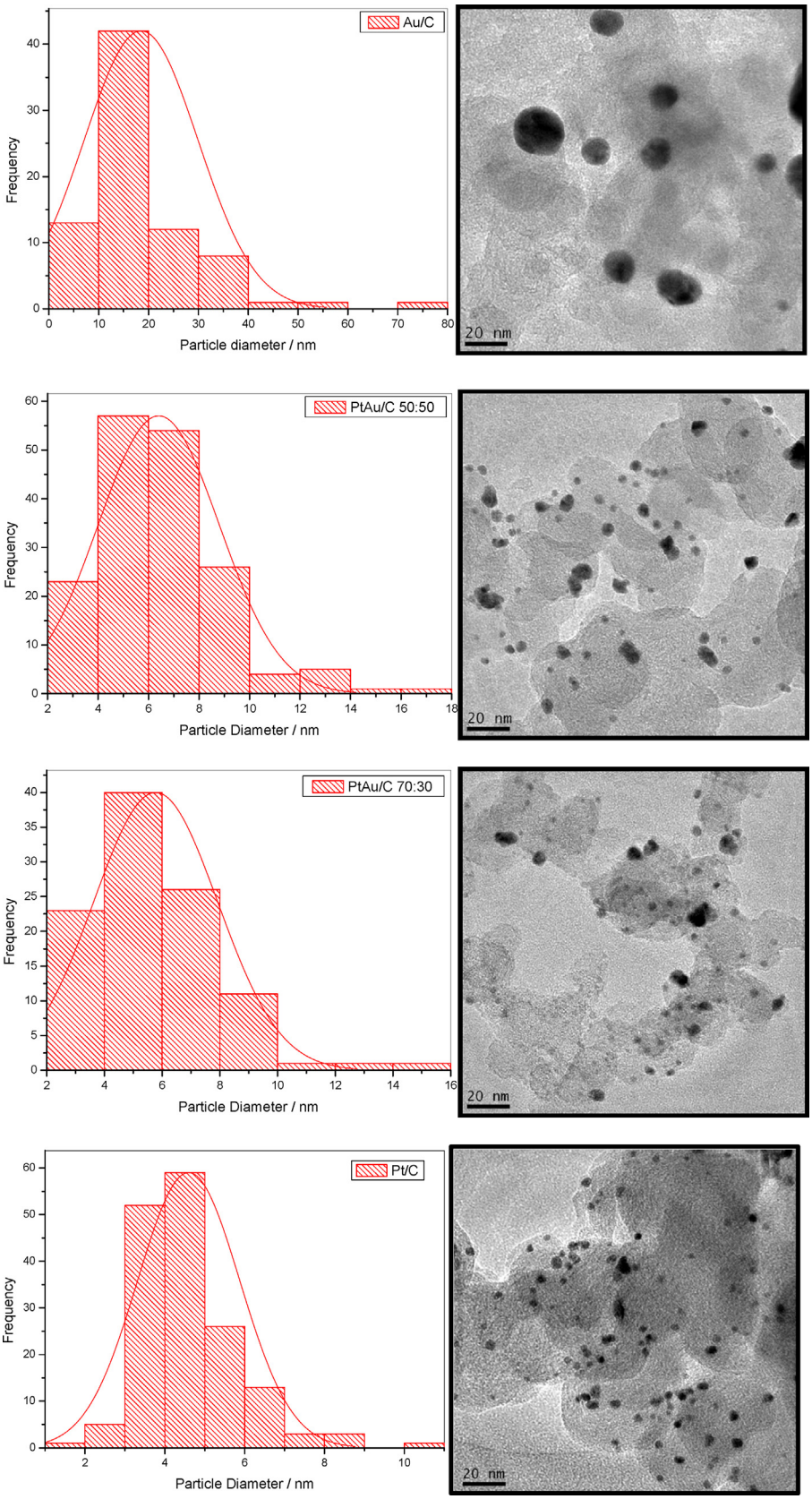

Fig. 2. TEM micrographs of Au/C and PtAu/C electrocatalysts and their respective histograms.

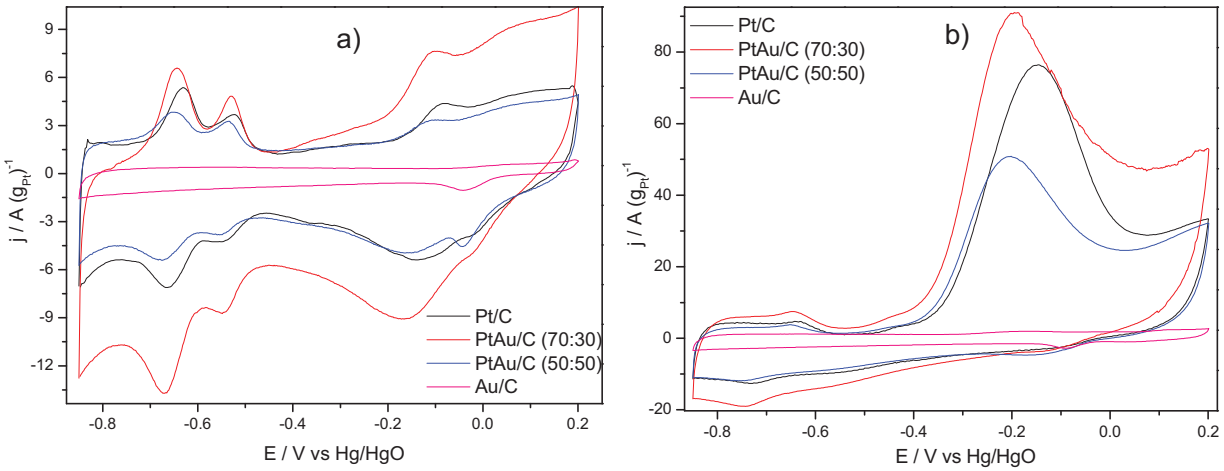

Fig. 3. (a) Voltammograms of Pt/C, PtAu/C (70:30), PtAu/C (50:50) and Au/C in 1 moL L^{-1} KOH at 20 mV s^{-1}; (b) voltammograms of Pt/C, PtAu/C (70:30), PtAu/C (50:50) and Au/C in 1 moL L^{-1} KOH + 1 mol L^{-1} NH_4OH at 20 mV s^{-1}.

The voltammetry results performed at 1 mol L^{-1} KOH and on 1 mol L^{-1} NH_4OH + 1 mol L^{-1} KOH at 20 mV s^{-1} are displayed on Fig. 3a and b, respectively. From Fig. 3a it is possible to observe a well-defined region of hydrogen adsorption/desorption at −0.85 to −0.45 V on PtAu/C and Pt/C electrocatalysts evidencing the presence of Pt [32]. Additionally, one more peak was identified in the region of −0.1 and 0.05 V what could be attributed to the adsorption of OH^- species [31]. Moreover, a peak at about −0.04 V during negative scan could be attributed to the reduction of gold species [33,34].

Fig. 3b shows a well-defined anodic current peak around −0.20 V (HgHgO) which is attributed to the oxidation of ammonia [12,21], confirming the activity of PtAu electrocatalysts toward ammonia oxidation. It is important to stress that among all electrocatalysts in study, PtAu/C (70:30) showed the highest peak current, which was about 20% higher than the obtained with Pt/C. Au/C showed to be inactive toward ammonia oxidation.

According to de Vooys et al. [17] gold has low dehydrogenation capacity or weak affinity for N_{ads} and so do not have the ability to produce N_2. In this paper, they affirm that only platinum and iridium electrodes exhibit steady-state N_2 production at potentials at which no surface oxide are formed. Nevertheless Pt shows higher affinity to N_{ads} which is responsible to the lower activity toward ammonia oxidation.

In a next work, de Vooys et al. [35] using gold electrodes toward ammonia electro-oxidation showed (considering differential electrochemical mass spectroscopy experiments) that on Au electrodes there is the formation of N_2O.

Considering binary electrodes composed of Pt and Au it is known that the first metal has excellent ability for ammonia dehydrogenation however the production of N_{ads} on its surface is responsible for the deactivation of Pt electrodes at higher potentials [17]. However, Au has low affinity for N_{ads}. Thus it is expected that the introduction of Au in Pt electrodes could be a good alternative for the ammonia oxidation as observed on Figs. 3 and 4.

Fig. 4 shows the chronoamperometry obtained at −0.300 V (vs HgHgO). From this figure it is possible to affirm that Pt/C and PtAu/C (70:30) showed almost the same final current to PtAu/C (70:30), however the PtAu/C (70:30) showed to be more stable than Pt/C since its decrease in current density was not so evidenced as Pt/C. Additionally, Au/C shows no active toward ammonia oxidation in chronoamperometric experiments.

Fig. 5 shows the polarization and power density curves using 1.0, 3.0 and 5.0 mol L^{-1} NH_4OH in 1 mol L^{-1} KOH as fuels, Pt/C, Au/C and PtAu/C catalysts as anode in a DAFC operated at 40 °C, using also Pt/C BASF as cathode for all experiments. The results obtained from DAFC are summarized in Table 1.

In all concentrations of NH_4OH studied, the best electrocatalysts used was the PtAu/C (70:30). This electrocatalyst showed a power density about 60% higher than Pt/C in all concentration of NH_4OH analyzed and among the fuel concentrations the NH_4OH 5 mol L^{-1} in 1 mol L^{-1} KOH showed the best results.

From Fig. 5 it is also possible to observe that the highest OCVs were obtained with PtAu/C (70:30) which are significantly higher than the ones obtained with Au/C and Pt/C. This difference in OCV reflects the catalytic activity of each catalyst for NH_4OH oxidation [36].

While gold has been demonstrated to be chemically most inactive among noble metals due to its electronic configuration, gold metal finely dispersed on metal oxides has been demonstrated to be a promising catalyst in a number of catalytic reactions. Thus, supported Au catalysts are promising catalysts in various areas [30].

Yan and Zhang [37] studied the methanol oxidation in alkaline media using Au/C and showed that the methanol oxidation current enhances with the decrease of the average size of Au nanoparticles. Zhang et al. [38] used gold electrode for oxidation of ammonia borane and showed that gold could contribute to the formation of adsorbed hydroxyl species $AuOH_{ads}$ which is believed to have catalytic properties for oxidation reactions of other species in solution.

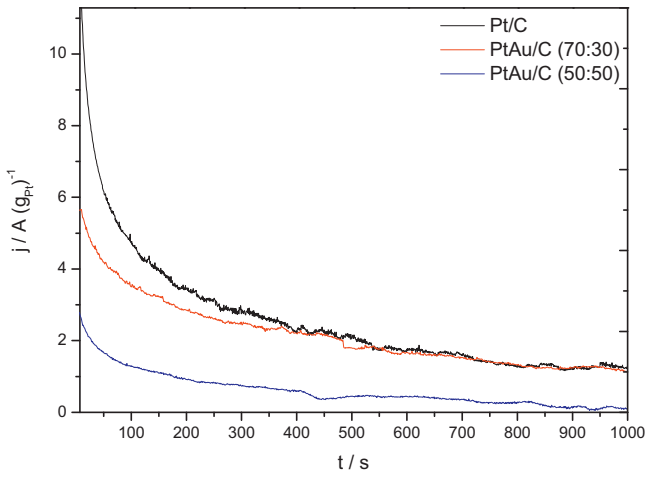

Fig. 4. Chronoamperometric results at −0.30 V for Pt/C, PtAu/C (70:30), PtAu/C (50:50) and Au/C in 1 moL L^{-1} KOH + 1 mol L^{-1} NH_4OH.

Table 1
The main results of DAFC experiments.

Catalyst	NH_4OH 1 mol L^{-1}		NH_4OH 3 mol L^{-1}		NH_4OH 5 mol L^{-1}	
	OCV/V	P_{max} (mW cm^{-2})	OCV/V	P_{max} (mW cm^{-2})	OCV/V	P_{max} (mW cm^{-2})
Au/C	0.289	0.516	0.270	0.486	0.263	0.492
Pt/C	0.458	1.47	0.478	1.64	0.470	1.64
PtAu/C 50:50	0.508	2.06	0.482	1.95	0.450	1.76
PtAu/C 70:30	0.584	2.33	0.581	2.51	0.588	2.64

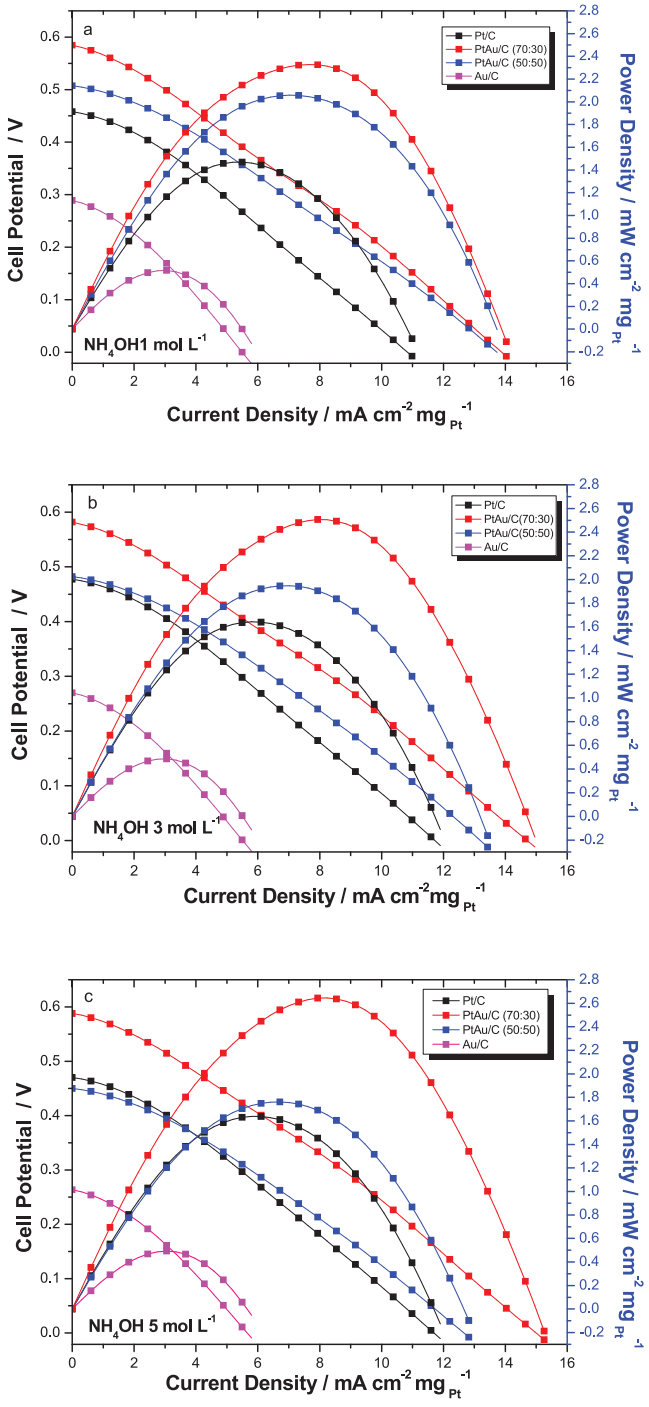

Fig. 5. Polarization and power density curves of a 5 cm^2 DAFC at 40 °C using (a) NH_4OH 1.0 mol L^{-1}; (b) NH_4OH 3.0 mol L^{-1} and (c) NH_4OH 5.0 mol L^{-1}, all in KOH 1 mol L^{-1}.

According to de Vooys et al. [35], platinum shows a good dehydrogenation capacity. However, considering their DFT calculations, Pt shows an N adsorption energy of −394 kJ mol^{-1} while Au shows an N adsorption energy of −162 kJ mol^{-1}. Thus, in PtAu/C electrocatalysts, Au could contribute to the decrease of poisoning on catalysts surface by N_{ads} species, facilitating the ammonia oxidation [12,18].

Taking into account that the Pt:Au/C (70:30) also showed the lower mean diameter size, the best result obtained with this material could be attributed to the lower particle size associated with the presence of an enhanced synergic effect for this specific metal ratio [39,40]. Thus, Pt:Au/C (70:30) showed an expansion of the lattice parameter, suggesting the formation of PtAu alloy might cause weakening of the metal–N_{ads} bond strength leading to a decrease in the surface poisoning and facilitating ammonia oxidation [12]. Also, the presence of $AuOH_{ads}$ species could also contribute to the ammonia oxidation [38].

4. Conclusions

The borohydride method was efficient for the preparation of PtAu electrocatalysts, yielding PtAu/C electrocatalyst with mean average size of about 6 nm. Among the PtAu/C materials studied, the PtAu/C (70:30) showed the lowest mean crystallite size and also the best results toward ammonia oxidation reaction. In electrochemical experiments PtAu/C (70:30) showed a current density 20% higher than the obtained for Pt/C while in DAFC experiments PtAu/C (70:30) showed a power density almost 60% higher than the obtained with Pt/C in all NH_4OH concentrations. PtAu/C (70:30) showed an expansion of the lattice parameter, indicative of the PtAu alloy formation that could contribute for ammonia electrooxidation by the electronic effect. Furthermore, Au could contribute to the decrease of poisoning on catalysts surface by N_{ads} species since it presents lower N adsorption energy than Pt. Thus, Au could also form $AuOH_{ads}$ species which could also contribute to the higher power density obtained by the PtAu/C (70:30).

Acknowledgments

The authors wish to thank Laboratório de Microscopia do Centro de Ciências e Tecnologia de Materiais (CCTM) by TEM measurements, FAPESP (2013/01577-0, 2011/18246-0, 2012/22731-4, 2012/03516-5) and CNPq (150639/2013-9, 141469/2013-7) for the financial support.

References

[1] M. Belén Molina Concha, M. Chatenet, F.H.B. Lima, E.A. Ticianelli, Electrochim. Acta 89 (2013) 607–615.
[2] S. Sharma, B.G. Pollet, J. Power Sources 208 (2012) 96–119.
[3] E. Antolini, E.R. Gonzalez, J. Power Sources 195 (2010) 3431–3450.
[4] S.A. Hajimolana, M.A. Hussain, W.M.A.W. Daud, M.H. Chakrabarti, Chem. Eng. Res. Des. 90 (2012) 1871–1882.
[5] A. Allagui, S. Sarfraz, E.A. Baranova, Electrochim. Acta 110 (2013) 253–259.
[6] A.A. Boretti, Int. J. Hydrogen Energy 37 (2012) 7869–7876.
[7] S. Appari, V.M. Janardhanan, S. Jayanti, L. Maier, S. Tischer, O. Deutschmann, Chem. Eng. Sci. 66 (2011) 5184–5191.
[8] S.F. Yin, B.Q. Xu, X.P. Zhou, C.T. Au, Appl. Catal. A: Gen. 277 (2004) 1–9.
[9] S.-F. Yin, B.-Q. Xu, S.-J. Wang, C.-T. Au, Appl. Catal. A: Gen. 301 (2006) 202–210.

[10] J. Zhang, H. Xu, X. Jin, Q. Ge, W. Li, Appl. Catal. A: Gen. 290 (2005) 87–96.
[11] Z. Wang, Z. Qu, X. Quan, H. Wang, Appl. Catal. A: Gen. 411–412 (2012) 131–138.
[12] T.L. Lomocso, E.A. Baranova, Electrochim. Acta 56 (2011) 8551–8558.
[13] B.K. Boggs, G.G. Botte, Electrochim. Acta 55 (2010) 5287–5293.
[14] L.A. Diaz, A. Valenzuela-Muñiz, M. Muthuvel, G.G. Botte, Electrochim. Acta 89 (2013) 413–421.
[15] M.H.M.T. Assumpção, S.G. da Silva, R.F.B. de Souza, G.S. Buzzo, E.V. Spinacé, A.O. Neto, J.C.M. Silva, Int. J. Hydrogen Energy 39 (2014) 5148.
[16] M.H.M.T. Assumpção, S.G. da Silva, R.F.B. de Souza, G.S. Buzzo, E.V. Spinacé, M.C. Santos, A.O. Neto, J.C.M. Silva, J. Power Sources 268 (2014) 129.
[17] A.C.A. de Vooys, M.F. Mrozek, M.T.M. Koper, R.A. van Santen, J.A.R. van Veen, M.J. Weaver, Electrochem. Commun. 3 (2001) 293–298.
[18] M.H.M.T. Assumpção, S.G. da Silva, R.F.B. de Souza, G.S. Buzzo, E.V. Spinacé, A.O. Neto, J.C.M. Silva, Int. J. Hydrogen Energy 39 (2014) 5148–5152.
[19] R.S. Henrique, R.F.B. De Souza, J.C.M. Silva, J.M.S. Ayoub, R.M. Piasentin, M. Linardi, E.V. Spinace, M.C. Santos, A.O. Neto, Int. J. Electrochem. Sci. 7 (2012) 2036–2046.
[20] A.O. Neto, M.M. Tusi, N.S. de Oliveira Polanco, S.G. da Silva, M. Coelho dos Santos, E.V. Spinacé, Int. J. Hydrogen Energy 36 (2011) 10522–10526.
[21] X.T. Du, Y. Yang, J. Liu, B. Liu, J.B. Liu, C. Zhong, W.B. Hu, Electrochim. Acta 111 (2013) 562–566.
[22] H. Hou, S. Wang, W. Jin, Q. Jiang, L. Sun, L. Jiang, G. Sun, Int. J. Hydrogen Energy 36 (2011) 5104–5109.
[23] R.M. Modibedi, T. Masombuka, M.K. Mathe, Int. J. Hydrogen Energy 36 (2011) 4664–4672.
[24] H. Wang, Z. Liu, S. Ji, K. Wang, T. Zhou, R. Wang, Electrochim. Acta 108 (2013) 833–840.
[25] J. Tayal, B. Rawat, S. Basu, Int. J. Hydrogen Energy 36 (2011) 14884–14897.
[26] T.A. Yamamoto, T. Nakagawa, S. Seino, H. Nitani, Appl. Catal. A: Gen. 387 (2010) 195–202.
[27] W. Zhou, M. Li, L. Zhang, S.H. Chan, Electrochim. Acta 123 (2014) 233–239.
[28] T. Herranz, S. García, M.V. Martínez-Huerta, M.A. Peña, J.L.G. Fierro, F. Somodi, I. Borbáth, K. Majrik, A. Tompos, S. Rojas, Int. J. Hydrogen Energy 37 (2012) 7109–7118.
[29] D.N. Oko, J. Zhang, S. Garbarino, M. Chaker, D. Ma, A.C. Tavares, D. Guay, J. Power Sources 248 (2014) 273–282.
[30] H. Liu, A.I. Kozlov, A.P. Kozlova, T. Shido, K. Asakura, Y. Iwasawa, J. Catal. 185 (1999) 252–264.
[31] A.N. Geraldes, D.F. da Silva, E.S. Pino, J.C.M. da Silva, R.F.B. de Souza, P. Hammer, E.V. Spinacé, A.O. Neto, M. Linardi, M.C. dos Santos, Electrochim. Acta 111 (2013) 455–465.
[32] S.G. da Silva, J.C.M. Silva, G.S. Buzzo, R.F.B. De Souza, E.V. Spinacé, A.O. Neto, M.H.M.T. Assumpção, Int. J. Hydrogen Energy 39 (2014) 10121–10127.
[33] G. Chen, Y. Li, D. Wang, L. Zheng, G. You, C.-J. Zhong, L. Yang, F. Cai, J. Cai, B.H. Chen, J. Power Sources 196 (2011) 8323–8330.
[34] X. Hu, X. Shen, O. Takai, N. Saito, J. Alloys Compd. 552 (2013) 351–355.
[35] A.C.A. de Vooys, M.T.M. Koper, R.A. van Santen, J.A.R. van Veen, J.Electroanal. Chem. 506 (2001) 127–137.
[36] S. Suzuki, H. Muroyama, T. Matsui, K. Eguchi, J. Power Sources 208 (2012) 257–262.
[37] S. Yan, S. Zhang, Int. J. Hydrogen Energy 36 (2011) 13392–13397.
[38] X.-B. Zhang, S. Han, J.-M. Yan, H. Shioyama, N. Kuriyama, T. Kobayashi, Q. Xu, Int. J. Hydrogen Energy 34 (2009) 174–179.
[39] J.C.M. Silva, B. Anea, R.F.B. De Souza, M.H.M.T. Assumpção, M.L. Calegaro, A.O. Neto, M.C. Santos, J. Braz. Chem. Soc. 24 (2013) 1553–1560.
[40] D. Mott, J. Luo, P.N. Njoki, Y. Lin, L. Wang, C.-J. Zhong, Catal. Today 122 (2007) 378–385.